Design considerations for a new beamline for standard EXAFS at a high-energy low-emittance storage ring

Edmund Welter

Deutsches Elektronen-Synchrotron, A Research Centre of the Helmholtz Association, Notkestrasse 85, 22607 Hamburg, Germany. E-mail: edmund.welter@desy.de

P65 is a new EXAFS beamline to be built at the PETRA III storage ring at DESY in Hamburg. It will mainly be used for standard EXAFS applications with a relatively large beam and moderate flux density. While the beamline optics will be similar to many other standard EXAFS beamlines, the insertion device at such a large high-energy storage ring with low emittance like PETRA III will need special attention. This paper discusses the main design considerations for the construction of such a beamline at a 6 GeV storage ring with an emittance of 1 nm rad.

Keywords: EXAFS spectra quality; small emittance; source properties.

1. Introduction

From 22 October 2012 on, after about 40 years of operation, the DORIS III storage ring at Deutsches Elektronen Synchrotron (DESY) in Hamburg, Germany, will no longer be used as a source of synchrotron radiation. Since 1992 the DORIS storage ring has been operated as a dedicated synchrotron radiation source. DORIS III hosted about 40 different experiments, among them three dedicated EXAFS bending-magnet beamlines. These three beamlines currently cover the energy range between 2.4 keV and 100 keV. The typical beam size on the sample is between 1 mm × 1 mm and 1 mm × 10 mm (v × h) with an integral flux between 10^9 and 5×10^{10} s^{-1}.

Applications at these beamlines stem from different fields of science such as catalysis research, material sciences, biology, environmental sciences, geosciences, *etc*. The largest share of the available beam time is currently used for applications from chemistry, especially catalysis research. Many users are using EXAFS in a way very similar to standard methods in an analytical laboratory. This means that the users of the beamline are mainly interested in their respective analytical question and use EXAFS following more or less established standardized procedures as a tool that produces the required answer to an analytical problem. Together the overbooked beamlines provide more than 15000 h of beam time per year for external users. After the shutdown of DORIS III the beam time available at dedicated XAFS beamlines in Germany will be reduced to a quarter of the currently available number of hours and even on a European scale the available beam time for 'standard' XAFS experiments will be significantly reduced.

Therefore two new EXAFS beamlines will be built at DESY's PETRA III storage ring to compensate for the loss of EXAFS beam time. Both new beamlines will start user operation in summer/autumn 2014. PETRA III is a large third-generation storage ring with 2.3 km circumference operated at 6 GeV in top-up mode having a horizontal emittance of 1 nm rad. One of the two planned XAFS beamlines (P64) will provide a very high photon flux of 10^{12}–10^{13} s^{-1}. It will mainly be used for new experiments previously not feasible at DESY, like quick-scanning EXAFS with 20–50 Hz repetition rate (Stötzel *et al.*, 2010), measurements in highly diluted samples, and flux-hungry applications like resonant or non-resonant inelastic X-ray scattering. This beamline will use moderate focusing to beam diameters around 100 µm. An even smaller beam will be provided for those applications that need it at a third beamline (P63) which will also offer the possibility to measure EXAFS spectra.

The intention of beamline P65 is to provide a new 'work-horse beamline' for the existing large DORIS III user community. These applications do not need a small beam size or extremely high flux, on the contrary they are often complicated by these beam properties. To serve this user community P65 will provide: (i) a large (1 mm × 1 mm to 1 mm × 2 mm) beam on the sample; (ii) a photon flux of 10^{10} s^{-1} to 10^{11} s^{-1}; (iii) an energy working range of 4 keV to 44 keV covering the *K* and *L* absorption edges, respectively, of the relevant elements; (iv) infrastructure for *in situ* applications; (v) simple standard procedures for inexperienced users.

This paper will discuss the technical design of beamline P65 and its potential impact on EXAFS data quality. The focus will be on the selection of the best suited source for the beamline, because this is the one beamline component which has the most significant influence on the XAFS spectra quality at beamline P65. The beamline optics consists of well tested

components and is very similar to XAFS beamline set-ups at other storage ring facilities.

2. Beamline set-up

2.1. Source

The ideal source for EXAFS experiments emits a broad and continuous spectrum. The beam on the sample should not show any spatial intensity distribution, especially no periodically variable intensity distribution. Bending magnets and bending-magnet-like insertion devices like wavelength shifters are therefore ideal sources for standard EXAFS applications. At the PETRA III storage ring, with its circumference of 2.3 km, their use is, however, impossible because of their relatively large divergence on the one hand and the long distance between the source and the first optical element ($\sim$50 m) on the other. Moreover, because of their large bending radius the critical energy of a standard PETRA III bending magnet in the existing ring lattice is <2 keV, making them unsuited to hard X-ray spectroscopy. This would have made it necessary to replace the standard dipoles with dipoles with a shorter bending radius in order to use them as a source for hard X-ray XAFS spectroscopy.

Instead it is now planned to replace the existing electron optics in the sector of the storage ring that will be used for the XAFS beamlines by a double-bend achromat (DBA) set-up, very similar to the electron optics in the already used sector of the storage ring (Franz *et al.*, 2006). The new design provides 5 m-long straight sections, divided by a small bending magnet into two 2 m-long sections for the installation of two canted insertion devices such as wigglers or undulators.

2.1.1. Wigglers. A classical wiggler emits a broad bending-magnet-like spectrum that makes it a well suited source for XAFS spectroscopy. Wigglers are foreseen as a source of synchrotron radiation for many of the new third-generation sources working in the 3 GeV electron energy range (*e.g.* I20 at Diamond, Claess at ALBA, to name just the European ones). They usually have a deflection parameter (K) of between 10 and 15, that results in a critical energy of 15–20 keV and a tolerable heat load on the first optical component. Apparently they deliver a smooth beam profile without energy-dependent spatial fluctuations (Diaz-Moreno, 2012; Klementev, 2012).

However, a device with a K value above 10 is difficult to use at a storage ring like PETRA III, which is operated at an electron energy of 6 GeV, firstly because of the extreme heat load it produces and secondly because of its high critical energy. Actually the maximum tolerable integral heat load of 1 kW on the currently available beamline front-end components limits a possible wiggler at PETRA III to a maximum K of between 6 and 10 depending on the length of the device.

Simulations of the spectral properties of wigglers with K values between 6 and 10, operated at a 6 GeV machine with 1 nm rad emittance, which were performed using the *SRW* (Chubar & Elleaume, 1998) and *SPECTRA* (Tanaka & Kitamura, 2001) codes, show distinct energy-dependent inter-
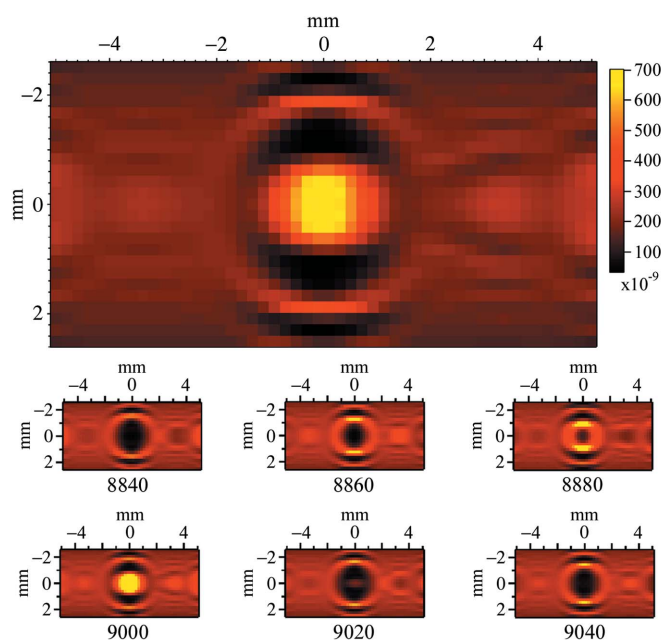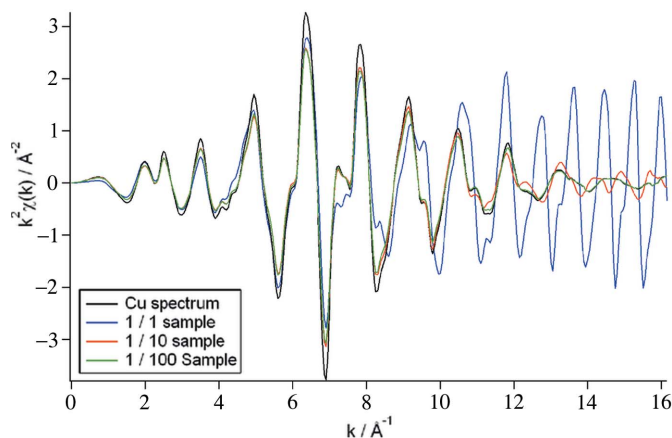

Figure 1
Intensity distribution of the radiation from a four-period wiggler with K = 6 and 200 mm period length on the sample, calculated for different energies between 8840 eV and 9040 eV. The large plot shows the intensity variation at 8900 eV; the difference between dark and bright areas is about a factor of 20.

ference effects that result in strong periodic changes of the spatial intensity distribution, very similar to those observed at (tapered) undulators during an XAFS scan. Fig. 1 shows simulated plots of the spatial intensity distribution at several energies between 8840 and 9040 eV, emitted from a four-period wiggler with K = 6, a period length of 200 mm and a resulting critical energy of 7898 eV. During an energy scan the observed maxima and minima move periodically over the sample. The number of periods was limited to four to stay below the maximum allowed power load density of the first optical component. The intensity profiles are, however, pretty similar for longer insertion devices.

Depending on the homogeneity of the sample this behaviour can cause severe artefacts in the measured absorption spectra which render them unusable for further analysis. Fig. 2 presents the results of a simulation of the expected effects on the spectra of more or less inhomogeneous Cu samples. The simulated spectra were generated by calculating the transmitted number of photons at each pixel of the 'samples' and summing them up to calculate the integral number of transmitted photons I_t. With the number of incoming photons being I_0, the absorption at a certain energy point is then simply calculated as $-\ln(I_t/I_0)$.

It is obvious that the periodic changes of the intensity distribution during an EXAFS scan can cause severe artefacts, especially in the case of samples with inhomogeneities on a length sale comparable with the length scale of the intensity changes (see the 'sample' on the upper right in Fig. 2). The exact frequency and amplitude of the intensity fluctuations are a function of the insertion device parameters, but are poten-

Figure 2
Simulated EXAFS spectra of Cu 'samples' with varying degrees of inhomogeneity. For the small plots on the right the upper 'sample' has a 'grain size' of 0.25 mm × 0.25 mm, the middle and lower 'samples' have 10 times and 100 times, respectively, smaller 'grain size'. The intensity distributions used in the simulation are those shown in Fig. 1. They were calculated for a wiggler with $K = 6$ installed in the PETRA III storage ring.

tially very close to the frequency and amplitude of the EXAFS oscillations.

2.1.2. Undulators. Undulators provide the highest possible brilliance and, more important for XAFS, flux. If the undulator gap is tuned so that the used energy is emitted by one of the odd harmonics, most of the intensity is concentrated in the narrow central cone. The intensity profile of this cone is symmetric and, provided that the undulator gap is tuned synchronously to the monochromator, the profile does not change significantly if the energy is changed over the course of the EXAFS scan.

The chosen type of double-crystal monochromator (DCM) and the use as a source for long energy scans impose some restrictions on the undulator. The most important is the maximum allowed power load on the optical elements. In the case of P65 the limit is set by the first monochromator crystal. The power load density on this indirectly water-cooled crystal must not exceed 2 W mm^{-2} under normal incidence. The second important requirement is the necessary long overlap between the first and third undulator harmonic. This overlap must be large enough to finish an EXAFS scan for element Z on the first and start EXAFS scans on element $Z + 1$ on the third harmonic (see Fig. 3). Using a water-cooled mirror as a low-pass filter in front of the DCM the best compromise between the partly contradicting requirements is an insertion device with 12 periods, a period length (λ_U) of 32.0 mm and a maximum K of 2.6 (minimum magnetic gap 10.05 mm). This insertion device covers the entire energy range between 4 keV and 44 keV; it allows Fe K-edge EXAFS to be finished using the first undulator harmonic and to start Co K-edge EXAFS using the third undulator harmonic. If needed at some later time the energy range between 2.4 and 4 keV is in principle accessible; the mechanical limit of the magnetic gap is 9.5 mm.

The undulator gap and the DCM will be scanned continuously to minimize the mechanical wear and scan time overhead. The expected time needed to perform one full transmission-mode EXAFS scan ($\Delta E = 1200$ eV) will be

between 1 and 5 min. This value is estimated from the expected flux on the sample. Ray-tracing calculations, that included the reflectivity of two mirrors and the absorption by two diamond windows, using the *XOP* and *Shadowvui* codes (Sanchez del Rio & Dejus, 1997), yielded a monochromatic photon flux between 0.24×10^{11} s^{-1} and 31×10^{11} s^{-1} on the sample, depending on the energy and the configuration of the beamline (see Table 1).

First tests at one of the existing undulator beamlines at PETRA III (P06) showed that synchronized gap/DCM scans are feasible with the existing beamline control system. The maximum deviation during a scan between 8.5 and 10 keV was smaller than 2 eV (Wellenreuther, 2012). Numerical simulations show that, even for very inhomogeneous or textured samples, this is already far better than necessary to avoid changes of the absorption $[-\ln(I_1/I_0)]$ of larger than 10^{-4} (see Table 2).

K as a function of the gap (g) was calculated for $\lambda_U = 32.0$ mm using equation (1) derived from Elleaume *et al.* (2000),
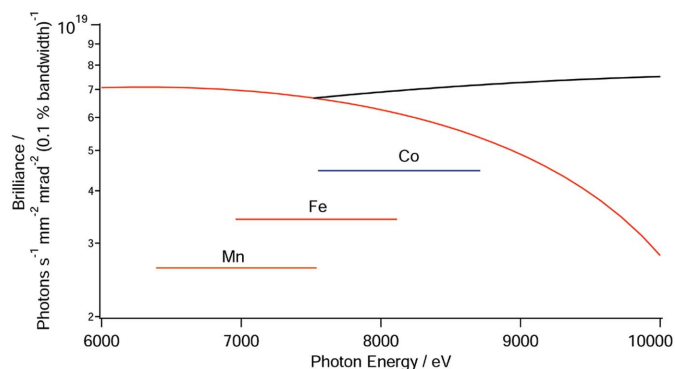
$$K = 0.345 \lambda_U \exp\left[-5.068(g/\lambda_U) + 1.52(g/\lambda_U)^2\right]. \quad (1)$$

The K value was then used to calculate the zero emittance energy E_p in keV using equation (2) (Tischer, 2010) with a storage ring energy E_M of 6 GeV,

$$E_p = \frac{0.950\, E_M}{\lambda_U(1 + K^2/2)}. \quad (2)$$

2.2. Beamline optics

The beamline optics of P65 is pretty similar to the set-up of many other EXAFS beamlines and basically consists of a

Figure 3
Brilliance of the used U32.0 undulator in the critical energy region between first and third undulator harmonic. The three horizontal lines show the scan ranges for Mn, Fe and Co EXAFS scans.

Table 1
Monochromatic photon flux through a 1 mm × 2 mm aperture at the sample position, calculated for different energies and beamline configurations (mirrors and DCM crystals) using *XOP/shadowvui*.

Set-up	Flux (s⁻¹)	Energy resolution (FWHM) (eV)
Si 111, 4000 eV, Ni, 7 mrad	9.2×10^{10}	0.41
Si 111, 9000 eV, Rh, 3 mrad	3.3×10^{11}	1.17
Si 311, 15000 eV, Rh, 3 mrad	5.4×10^{10}	1.02
Si 311, 25000 eV, Pt, 3 mrad	2.4×10^{10}	2.75

Table 2
Influence of gap position errors on the measured $-\ln(I_1/I_0)$ of two different inhomogeneous samples (see Fig. 5).

The gap of a U32.0 undulator stays tuned to a zero emittance energy of 9000 eV (third harmonic, $K = 2.1247$). The DCM energy (E) is varied.

			$-\ln(I_1/I_0)$	
E (eV)	Correct gap (mm)	I_0 [s⁻¹ (10^{-4} bandwidth)⁻¹]	Sample 1	Sample 2
8990	13.5724	1.28×10^{12}	0.38256	1.42535
8995	13.5760	1.26×10^{12}	0.38254	1.42536
9000	13.5796	1.24×10^{12}	0.38252	1.42537
9005	13.5832	1.21×10^{12}	0.38250	1.42539
9010	13.5868	1.18×10^{12}	0.38248	1.42540

stable DCM and two plane mirrors mounted in front of the DCM to reduce the power load of the first DCM crystal and for effective higher harmonics suppression. Fig. 4 provides a schematic overview of the set-up of beamline P65.

2.2.1. DCM. The DCM that will be installed at beamline P65 is already in use at several DORIS III beamlines. It is an indirectly water-cooled fixed-exit DCM with the option for a remotely controlled fast crystal change (Rickers *et al.*, 2007; Welter, 2010). At P65 it will be equipped with Si 111 and Si 311 crystal pairs. In this configuration the DCM covers the energy range between 2.4 keV and 44 keV.

Compared with cryogenically cooled DCMs, water-cooled DCMs have the advantage that it is easier to achieve mechanical stability. Their design and operation are relatively simple, making them well suited for a standard EXAFS beamline. This was proved, as far as this is possible on a bending-magnet beamline, for the DCM used, during commissioning and user operation at the DORIS III EXAFS beamlines A1 and C. The estimated power load density limit

of this DCM is ~2 W mm⁻², which is significantly lower than the respective limit for a cryogenically cooled DCM and limits the maximum length and thus flux of the undulator source. The exact value for the maximum tolerable power load density will be determined experimentally before a final decision about the undulator length is made.

The Bragg axis of the DCM is equipped with a Renishaw angle encoder with 2.24×10^{-6} deg resolution. The output of the encoder provides a very precise and highly reproducible energy axis for the EXAFS experiments and is used as the master signal for the above-mentioned synchronization between the movement of the Bragg axis and the tuning of the undulator gap.

2.2.2. Mirrors. The mirrors serve two main purposes, first to reduce the power load of the first DCM crystal and second to suppress higher harmonics radiation to achieve the high degree of spectral purity which is mandatory for XAFS spectroscopy. The demanded spot size in the 1 mm × 1 mm to 1 mm × 2 mm range can be achieved without focusing optics, therefore both mirrors will be plane mirrors. The first mirror is water-cooled. Effective higher harmonics suppression over the entire X-ray photon energy range between 4 keV and 44 keV is only possible by the combination of different mirror coatings and variable incidence angles. It is planned to use plane mirrors with Si, Rh and Pt stripes and adjustable incidence angles between 1.5 and 4.5 mrad. This design suppresses the third monochromator harmonic by a factor of 10^{-4} over the entire working range. At the same time the two mirrors are an effective means to reduce the power load on the first crystal. At higher energies using the fifth or higher undulator harmonics a water-cooled filter will be used in front of the first mirror to reduce the power load further. Mirror and filter together act as a bandpass filter. Table 3 gives an overview of the expected power load density on the first optical element behind a water-cooled mirror/filter combination.

3. Conclusion

The new EXAFS beamline P65 will be optimized for the demands of a user community that wants a relatively large beam with moderate photon flux to perform standard EXAFS experiments. The emphasis is to provide simple and stable operation. Whilst the design of the beamline optics (DCM and
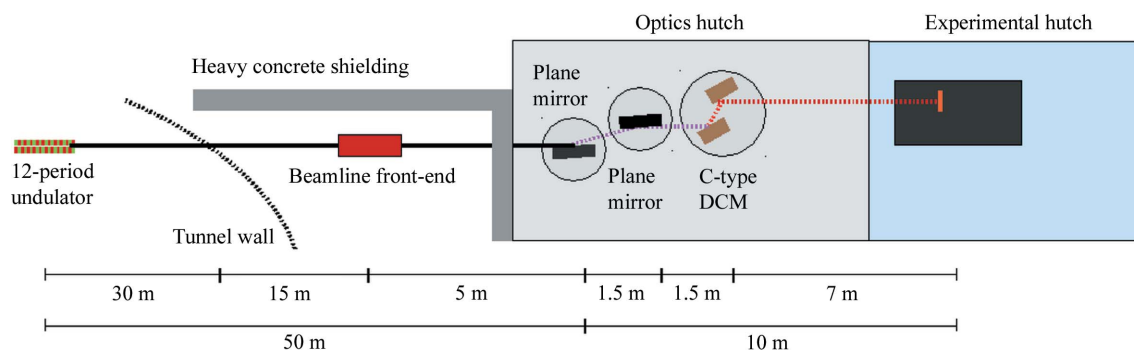
Figure 4
Schematic drawing of beamline P65; all dimensions are approximate.
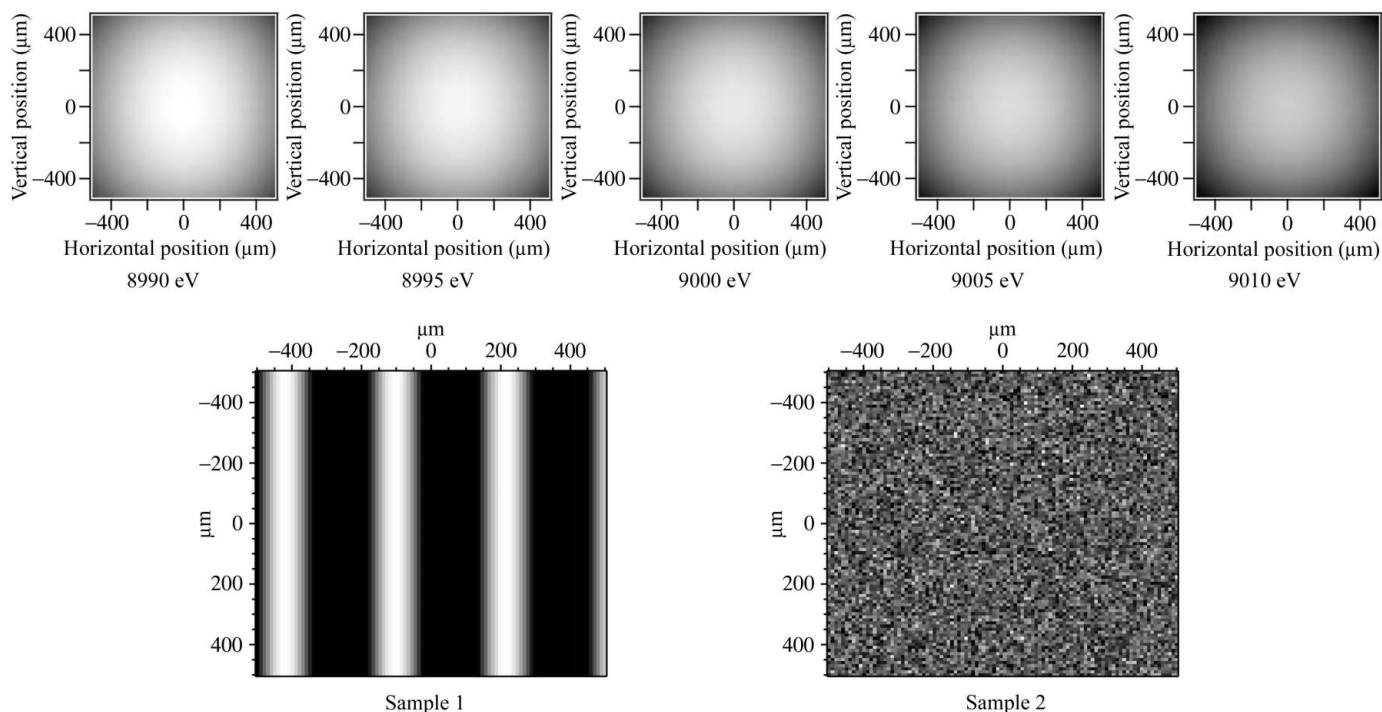
Figure 5
Upper row: intensity distribution I_0, photon flux density between white (1.4×10^{12} s^{-1}) and black (9.7×10^{11} s^{-1}) at different DCM energies. Undulator parameters: $\lambda_U = 32.0$ mm, length = 384 mm (12 periods), $K = 2.1247$ (9000 eV), distance = 60 m, 1 mm × 1 mm. Lower row: 'samples' used for the simulation of the influence of deviations of the undulator gap tuning from the DCM energy, 'grain' size 0.01 mm × 0.01 mm; sample 1, sinusoidal variation of the thickness (texture); sample 2, random variation of the thickness (powder).

Table 3
Power load on the first crystal of the C-type DCM at a distance of 50 m from a 12-period U32 undulator.

A plane mirror with variable angle of incidence acts as a low-pass filter; at higher X-ray photon energies it is combined with a cooled filter to form a bandpass filter. The calculated flux into 10^{-3} bandwidth includes the losses due to the mirror and filter.

E (eV)	K	Harmonic	Mirror	Filter	Power load (W mm^{-2})	Flux (× 10^{12} mm^{-2} s^{-1})
4000	1.867	1	Si 4 mrad	–	0.56	9.5
7516	2.600	3	Rh 4 mrad	–	1.22	8.9
15000	2.306	3	Rh 4 mrad	–	1.27	6.8
20000	2.384	7	Pt 3 mrad	C 0.5 mm	1.53	4.4
30000	1.767	7	Pt 2 mrad	C 2 mm	1.63	2.3
44000	1.578	9	Pt 1.8 mrad	C 2 mm	1.54	0.62
44000	1.867	11	Pt 1.8 mrad	C 2 mm	1.87	0.85

mirrors) for such a beamline is relatively simple and similar to standard EXAFS beamline set-ups, it turned out that the choice of the insertion device for the production of synchrotron radiation is complicated by the properties of the storage ring, namely the small emittance combined with the high electron energy. This can result in strong and periodically changing interference patterns in the photon beam.

This excludes wiggler-like devices with K values of around 6, while stronger wigglers with K values above 10 cannot be used owing to the enormous emitted power. Under these conditions a short undulator with $K_{max} = 2.6$ seems the best choice. For energy scans this device requires synchronized undulator gap and DCM scans. These scans are feasible with the required precision and speed. Insertion device parameters such as maximum K, period length, etc. are mainly determined by the maximum allowed power load on the first DCM crystal and by the requirement to perform long continuous energy scans.

The main components of the beamline optics of P65 will be a stable water-cooled DCM and a pair of plane mirrors with several coatings and adjustable incidence angle for higher harmonics suppression. The sample stage will be about 60 m away from the source. The expected flux on the sample will be between 10^{10} and 10^{11} photons s^{-1} in the monochromatic beam, depending on the energy.

References

Chubar, O. & Elleaume, P. (1998). *Proceedings of the Sixth European Particle Accelerator Conference (EPAC'98)*, Stockholm, Sweden, 22–26 June 1998, pp. 1177–1179.
Diaz-Moreno, S. (2012). Personal communication.
Elleaume, P., Chavanne, J. & Faatz, B. (2000). *Nucl. Instrum. Methods Phys. Res. A*, **455**, 503–523.

Franz, H., Leupold, O., Röhlsberger, R., Roth, S. V., Seeck, O. H., Spengler, J., Strempfer, J., Tischer, M., Viefhaus, J., Weckert, E. & Wroblewski, T. (2006). *Synchrotron Radiat. News*, **19**, 25–29.

Klementev, K. (2012). Personal communication.

Rickers, K., Brüggmann, U., Drube, W., Herrmann, M., Heuer, J., Welter, E., Schulte-Schrepping, H. & Schulz-Ritter, H. (2007). *AIP Conf. Proc.* **879**, 907–910.

Sanchez del Rio, M. & Dejus, R. J. (1997). *Proc. SPIE*, **3152**, 148–150.

Stötzel, J., Lützenkirchen-Hecht, D. & Frahm, R. (2010). *Rev. Sci. Instrum.* **81**, 073109.

Tanaka, T. & Kitamura, H. (2001). *J. Synchrotron Rad.* **8**, 1221–1228.

Tischer, M. (2010). *Forschung mit Synchrotronstrahlung*, edited by J. Falta and T. Möller, pp. 92–112. Wiesbaden: Vieweg and Teubner.

Wellenreuther, G. (2012). Personal communication.

Welter, E. (2010). *AIP Conf. Proc.* **1234**, 955–958.